Title

Temporal Optic Disc Microvasculature Dropout in Glaucoma

Journal

Investigative Ophthalmology & Visual Science, 64(11)

ISSN

0146-0404

Authors

Lim, Yeon Ju

Bang, Jong Wook

Weinreb, Robert N

et al.

Publication Date

2023-08-04

DOI

10.1167/iovs.64.11.6

Peer reviewed

Temporal Optic Disc Microvasculature Dropout in Glaucoma

Yeon Ju Lim,[1] Jong Wook Bang,[1] Robert N. Weinreb,[2] Linda M. Zangwill,[2] and Min Hee Suh[1]

[1]Department of Ophthalmology, Haeundae Paik Hospital, Inje University College of Medicine, Busan, South Korea
[2]Hamilton Glaucoma Center, Shiley Eye Institute, and the Viterbi Family Department of Ophthalmology, University of California San Diego, La Jolla, California, United States

Correspondence: Min Hee Suh, Department of Ophthalmology, Haeundae Paik Hospital, Inje University College of Medicine, 875 Haeundae-ro, Haeundae-gu, Busan 48108, South Korea; crishuna6@gmail.com.

Received: February 13, 2023
Accepted: July 6, 2023
Published: August 4, 2023

Citation: Lim YJ, Bang JW, Weinreb RN, Zangwill LM, Suh MH. Temporal optic disc microvasculature dropout in glaucoma. *Invest Ophthalmol Vis Sci.* 2023;64(11):6. https://doi.org/10.1167/iovs.64.11.6

Purpose. To assess the clinical characteristics of focal temporal optic disc microvasculature dropout (MvD-D) in primary open-angle glaucoma (POAG) patients.

Methods. One hundred and eighty-seven eyes of 187 POAG patients having MvD-D on Swept-Source optical coherence tomography angiography (SS-OCTA) were enrolled. Three groups were categorized according to the presence of temporal MvD-D within the upper and lower 45° of the fovea-Bruch's membrane (BM) opening axis: focal temporal MvD-D (Group 1, isolated focal temporal MvD-D; 44 eyes), supero/inferotemporal MvD-D (Group 2, MvD-D only in superotemporal or inferotemporal sector; 78 eyes), and diffuse temporal MvD-D (Group 3, MvD-D spanning ≥ 2 consecutive sectors, at least one of which being temporal sector; 65 eyes).

Results. Group 1 had a significantly longer axial length and β-zone parapapillary atrophy without BM. There also was a larger horizontal tilt angle and ovality index than the other two groups ($P < 0.001$). Group 1 had a significantly thinner retinal nerve fiber layer (RNFL) in the temporal sector than did Group 2 ($P < 0.001$), despite similar thicknesses in all other areas ($P > 0.05$). Group 3 had significantly worse visual field mean deviation and thinner RNFL than the other two groups in all areas other than the nasal, temporal, and superotemporal sectors ($P < 0.05$).

Conclusions. Focal temporal MvD-D detected by SS-OCTA was associated with a longer axial length and related subsequent morphological changes of the optic disc and parapapillary area. This suggests that stretching of the optic disc consequent on axial elongation may lead to absence of temporal optic disc microvasculature.

Keywords: myopia, optic disc microvasculature dropout, primary open-angle glaucoma

Glaucoma is a group of optic neuropathies characterized by progressive damage to the optic nerve head (ONH). Although multiple factors have been suggested as having a role in the pathogenesis of glaucoma,[1,2] ocular perfusion has been found to have significant relevance.[3,4] Specifically, lamina cribrosa (LC) and prelaminar tissue, putative sites of glaucomatous damage, both receive blood supply from the short posterior ciliary artery and the deep optic nerve circulation.[5–8] In this regard, optic disc microvasculature dropout (MvD-D), defined as absence of microvasculature within the deep ONH, was introduced as a useful parameter related to the pathogenesis of glaucoma.[9–12] However, it has been a challenge to assess the laminar and prelaminar capillaries because of shadowing or projection laid on the deeper tissue.

Meanwhile, swept-source optical coherence tomography angiography (SS-OCTA) facilitated visualization of the deep ONH microvasculature because it provides deeper penetration and includes removal of projection artifacts.[13,14] Moreover, the circumferential location of MvD-D can provide a clue to the pathogenesis of glaucomatous ONH damage. Several studies have demonstrated that eyes with focal LC defect in the temporal area tend to have myopia and damage to the retinal nerve fiber layer (RNFL) and visual field (VF) in the cecocentral area.[15,16] Given that MvD-D is closely related to that of focal LC defect,[9,13] eyes with MvD-D localized to the temporal area may also be associated with axial elongation and ONH change (i.e., deformation of the parapapillary region and axonal loss). However, there has been no study assessing the clinical features of glaucomatous eyes having focal temporal MvD-D. This study categorized the circumferential location of MvD-D by SS-OCTA and determined the factors associated with the presence of focal temporal MvD-D.

Methods

Study Subjects

This study included primary open-angle glaucoma (POAG) patients with MvD-D on optical coherence tomography angiography (OCTA) images. It was approved by the Institutional Review Board of Haeundae Paik Hospital, and written informed consent of the participants was waived.

All of the subjects underwent a complete ophthalmic examination, including best-corrected visual acuity,

refraction, slit-lamp biomicroscopy, intraocular pressure (IOP) measurement with Goldmann applanation tonometry, gonioscopy, fundus photography (TRCNW8; Topcon, Tokyo, Japan), as well as measurement of central corneal thickness (Ultrasound pachymetry; Oculus Optikgerate GmbH, Wetzlar, Germany), axial length (AXL) (IOL Master; Carl Zeiss Meditec, Dublin, CA, USA), and standard automated perimetry (Humphrey Field Analyzer 24-2 Swedish Interactive threshold algorithm standard; Carl Zeiss Meditec, Jena, Germany). Spectral-domain OCT (SD-OCT) and SS-OCTA images were acquired, all images and VF results being obtained within six months. Mean arterial pressure was calculated as one third of the systolic blood pressure (BP) plus two thirds of the diastolic BP (Model Easy X 800 [R/L]; Jawon Medical Co. Ltd., Kyungsan, Korea), and the mean ocular perfusion pressure was calculated as two thirds of the mean arterial pressure minus IOP. Optic disc hemorrhage, defined as an isolated splinter or flame-shaped hemorrhage on the optic disc, was determined by two masked observers (M.H.S. and Y.J.L.) based on fundus photographs and dilated fundus examination.

All subjects met the following inclusion criteria: diagnosed as POAG, open angle confirmed by gonioscopy, >18 years old, and best-corrected visual acuity ≥20/40. Those with a history of ocular surgery (except for uncomplicated cataract or glaucoma surgery) or any ocular or systemic conditions that could affect any study results were excluded. Subjects with diabetic mellitus or systemic hypertension were included if they did not have diabetic or hypertensive retinopathy. Both pre-perimetric and perimetric POAG with glaucomatous ONH damage (i.e., the presence of focal thinning, notching, localized or diffuse atrophy of the RNFL) were included. Perimetric POAG showed repeatable glaucomatous VF defects (i.e., outside the normal limit on glaucoma hemifield test, and/or pattern standard deviation (PSD) with a P value <0.05 on ≥2 consecutive reliable [fixation losses and false-negatives ≤33% and ≤15% false-positives) tests]).[17,18] Pre-perimetric POAG eyes did not show repeatable glaucomatous VF damage despite detectable glaucomatous optic disc damage.

OCTA

Angioplex OCTA (PLEX Elite 9000 Swept-Source OCT system; Carl Zeiss Meditec) with a projection artifact removal technique enables visualization of the vascular plexuses in various retinal layers that can be specified by the examiner. The FastTrac (Carl Zeiss Meditec) system was incorporated into the protocol for eliminating motion artifacts during image acquisition.[13,19–22] Eyes with poor-quality OCTA images (e.g., poor clarity, signal strength < 7, motion artifact) or poor visualization of the anterior laminar surface or choroidal or scleral layer (e.g., poor penetration of the OCT beam, shadowing of the neuroretinal rim or superficial vessels, segmentation error) were excluded (Fig. 1A).[13]

Determination of Presence and Location of Optic Disc and Parapapillary Deep-Layer Microvasculature Dropout

The two observers (M.H.S, and Y.J.L) masked to patient information and other ocular characteristics assessed the presence and location of the MvD-D and parapapillary microvasculature dropout (MvD-P) on the 6.0 × 6.0 mm ONH OCTA images. Disagreement between the two observers was discussed to reach a consensus; in cases where consensus could not be reached, the pertinent subject was excluded from the study.

MvD-D, defined as full-thickness absence of the prelaminar and laminar microvasculature within the optic disc, was assessed on both en-face and horizontal whole-signal-mode ONH OCTA images constructed from all of the OCTA signals below the internal limiting membrane (ILM) (Fig. 1C, Figs. 2A1, 2B12).[9,13] MvD-P was defined as full-thickness absence of the choriocapillaris or scleral microvasculature within the β-zone parapapillary atrophy (βPPA).[8,23,24] MvD-D and MvD-P were required to be detected in at least four consecutive horizontal B-scans and to be ≥200 µm in diameter on at least one scan (Fig. 1C).[8,9,13]

For determining the MvD-D and MvD-P, the temporal area of the vertical line ranging from the upper and lower 90° of the reference line connecting the fovea and Bruch's membrane opening (BMO) center (FoBMO axis) and passing through the optic disc centroid was used. The rationale for this approach is due to the fact that the nasal side of the deep optic nerve and PPA structure is hard to evaluate because of shadowing by the neural rim and large vessels.[9] The circumferential location of MvD-D and MvD-P was determined to be one of the following three sectors, using the FoBMO axis as the reference line:[15,25] temporal (T) (>315°–360°, > 0°–45°), superotemporal (TS) (>45°–90°) or inferotemporal (TI) (>270°–315°). If the MvD-D absence extended over ≥2 neighboring sectors, the sector containing the greater portion was selected. If the dropout was located in ≥2 consecutive sectors and each sector was equally involved, all of the sectors were assigned.[8,13,18]

According to the presence of MvD-D in the temporal sector, subjects were divided into three groups: focal temporal MvD-D (Group 1), supero/inferotemporal MvD-D (Group 2), and diffuse temporal MvD-D (Group 3). The focal temporal MvD-D group (Group 1) had isolated MvD-D in the temporal sector. This group could have MvD-D additionally in either the supero- or inferotemporal sector, but neither should be connected to the one in the temporal sector (Fig. 2A). The supero/inferotemporal MvD group (Group 2) had dropout only in the superotemporal and/or inferotemporal sector, sparing the temporal sector (Fig. 2B). The diffuse temporal MvD-D group (Group 3) had MvD-D spanning ≥2 consecutive sectors, at least one of which was the temporal sector (Fig. 3). If a patient's eyes met the criteria for different groups, they were categorized preferentially as, in order, focal temporal MvD-D (Group 1), diffuse temporal MvD-D (Group 3) or supero/inferotemporal MvD-D (Group 2), considering sparsity.

In addition to the qualitative analysis, optic disc vessel density (ODVD) was quantified by using publicly available ImageJ software (National Institutes of Health, Bethesda, Maryland, USA; http://imagej.nih.gov/ij/). The extracted en-face images were binarized using Otsu's method, which assumes that the image contains two classes of pixels following a bimodal distribution.[26–28] It calculates the optimum threshold by minimizing intraclass variance and maximizing interclass variance.[27,28] ODVD was calculated as the ratio of black pixels occupied by vessels divided by those from the region of interest (ROI).[26] ROI was determined as the cup area after excluding the neuroretinal rim area where the optic disc microvasculature is hardly visible due to shadowing in OCTA en-face image (Fig. 1).[10] The ODVD was measured by the two masked observers (M.H.S and

Investigative Ophthalmology & Visual Science

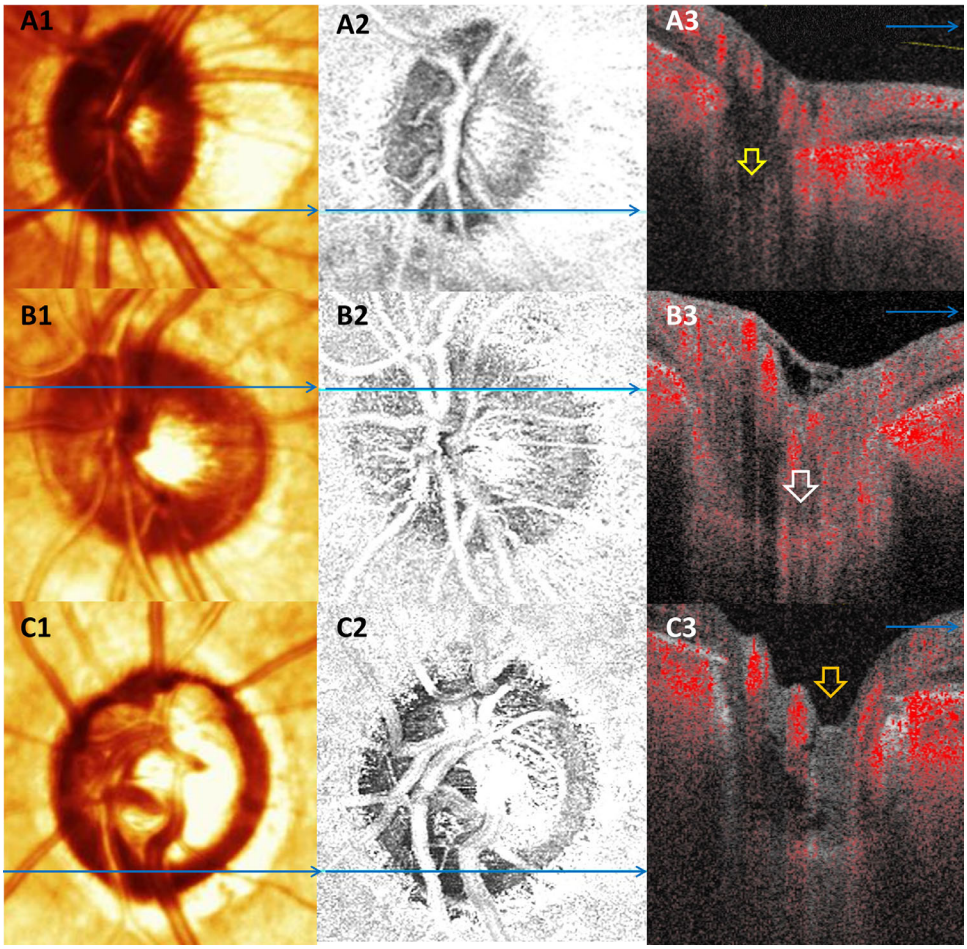

Figure 1. Representative cases showing differing visualization of the optic disc microvasculature under the neuroretinal rim area. A color-converted infrared fundus image (**A1, B1, C1**) and enface optical coherence tomography angiography (OCTA) (**A2, B2, C2**) with a line showing the level of horizontal B scan (**A3, B3, C3**). (**A**) Anterior laminar surface was not detectable because of shadowing of the neuroretinal rim and superficial vessels (*empty yellow arrow*). (**B**) Laminar microvasculature was visualized despite shadowing of the neuroretinal rim (*empty white arrow*). (**C**) Complete loss of OCTA signal was observed despite visible anterior laminar surface on the rim area was observed (*empty orange arrow*).

Y.J.L) on the global area and three sectors (T, TS, and TS) as mentioned above. The average of the two observers' measurements was used in the analysis.

OCT

RNFL thickness, BMO area, and βPPA width were assessed by Spectralis OCT2 Glaucoma Module Premium Edition software (version 1.9.17.0) (Spectralis; Heidelberg Engineering GmbH, Heidelberg, Germany) using 24 radial B scans aligned according to the FoBMO axis. RNFL thickness was calculated on a circle with a set diameter of 3.5mm in the global area and 6 sectors TS, TI, T, NS, NI, N) (Fig. 2A5 and B5). The average temporal widths of βPPA and βPPA$_{-BM}$, defined as the horizontal distance between the temporal optic disc boundary and the retinal pigment epithelium (RPE) and Bruch's membrane (BM) tips, respectively, were derived from radial B scans at the FoBMO axis by the two observers (J.W.B., Y.J.L.) (Fig. 2A3, A4 and B3, 4).[8,29–31] Temporal βPPA$_{+BM}$ width, defined as the horizontal distance between the temporal margin of the RPE and BM tips, was calculated as the difference between the βPPA and βPPA$_{-BM}$ widths. If the temporal margin of the ONH or βPPA was poorly visualized, adjacent radial scans located 15° apart were used for the assessment.[30]

Based on 20° × 20° enhanced depth imaging SD-OCT images composed of 48 radial B scans and color-converted infrared fundus images, optic disc tilt and torsion angle, ovality index, and presence of focal LC defect were determined by two observers (J.W.B., Y.J.L. for optic disc tilt and torsion angle, as well as ovality index, and M.H.S. and D.H.J. for presence of focal LC defect). Disagreements were resolved by consensus between the two observers. If consensus could not be reached, a third glaucoma specialist (M.H.S) served as an adjudicator. The average optic disc tilt and torsion angles were measured by the two observers using custom Matlab software (Matlab version 7.3.0.267; MathWorks, Natick, MA, USA). Focal LC defect was defined as laminar disinsertion or holes violating the normal shape.[15,16,32–35] To determine the sectoral location of the focal LC defect, three sectors (temporal, superotemporal, or inferotemporal) were derived by manually registering the large vessels on the enhanced depth imaging SD-OCT en face images to those on OCTA enface images.[13] If the focal LC defect was located in two consecutive sectors, only the sector that included the larger portion of the defect was assigned. If there were ≥2 sepa-

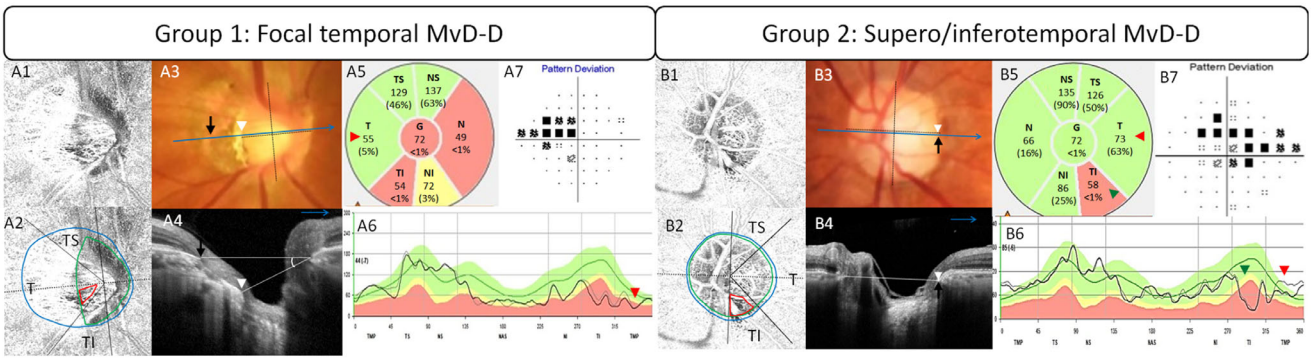

Figure 2. Representative cases showing differing clinical features of eyes categorized as focal temporal MvD-D (**A**) and supero/inferotemporal MvD-D (**B**) groups, respectively. **A2** and **B2** are the same images as **A1** and **B1**, but are labeled to indicate the 3 sectors from the fovea and Bruch's membrane opening (BMO) center axis (*black dotted lines*): T, TS, and TI; also indicated are the optic disc (*green circular lines*), and βPPA (*blue circular lines*) margins. The *large blue lines* (**A3, B3**) indicate the direction of the OCT scans (**A4**, **B4**). (**A**) MvD-D localized to temporal sector (*red circular lines* of **A2**) had an AXL of 27.8 mm. (**B**) MvD-D localized to inferotemporal sector (*red circular lines* of **B2**) had AXL of 24.4.mm. Note that an eye with focal temporal MvD-D (**A1, 2**) had longer βPPA without BM (the distance from the temporal optic disc margin [*white arrowheads*] to the BM tip [*black arrows*] [**A3, 4**]), larger ovality index (the ratio of the long axis to the short axis [*black dotted lines*] [**A3**]), and larger horizontal tilt angle (the angle between the line connecting both the BMO and the line connecting the nasal BMO and temporal optic disc margin [*white lines*] [**A4**]) than did an eye with inferotemporal MvD-D (**B1**). Also, an eye with focal temporal MvD-D had thinner retinal nerve fiber layer (RNFL) of the corresponding temporal sector (*red arrowheads* of **A5, 6**) than an eye with inferotemporal MvD-D having relatively preserved RNFL of the temporal sector (*red arrowheads* of **B5, 6**) despite remarkable RNFL thinning of the inferotemporal sector (*green arrowheads* of **B5, 6**). The two eyes had similar degrees of visual field damage (**A7**, **B7**).

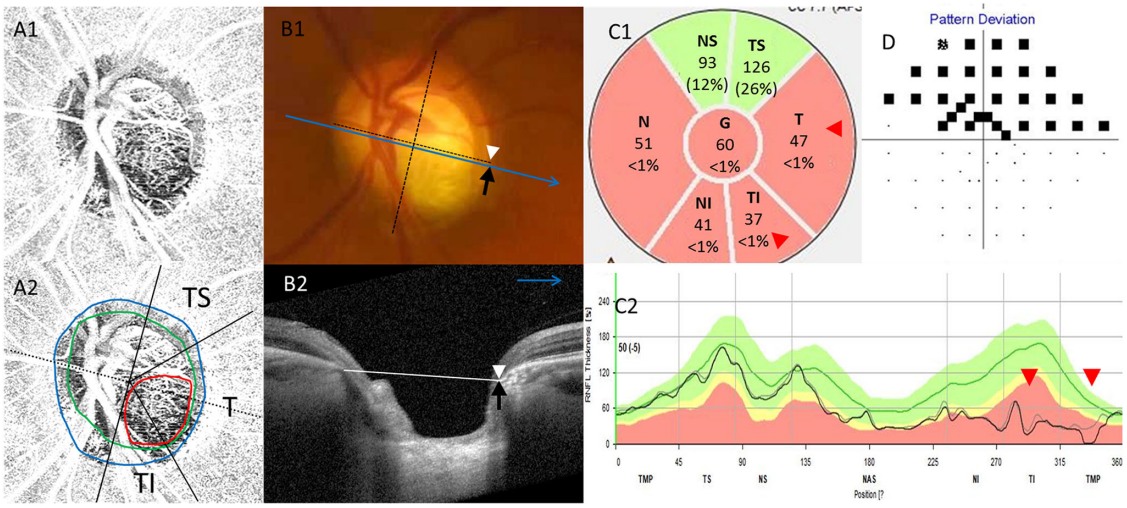

Figure 3. A representative case of an eye with MvD-D. **(A)** MvD-D located in the TI and T sectors had a normal range of axial length (22.2 mm). (**B**) The optic disc margin (*white arrowhead*) and BM tip (*black arrow*) were identical, suggesting that this eye was lack of β-zone parapapillary atrophy without BM (**B1, 2**) and horizontal tilt angle (*white line* [**B2**]). Ovality index measured as the ratio of the long axis to the short axis (*black dotted lines* [**B1**]) was relatively small (0.85). **C**, This eye had a thin retinal nerve fiber layer of the corresponding TI and T sectors (*red arrowheads* [**C1, 2**]). **D**, Visual field damage was observed in the corresponding superior hemifield.

rate focal LC defects, the location was determined for each of them. Optic disc tilt angle was determined as the angle between the reference plane connecting the two points of the BMO margin and the line connecting the nasal BMO and temporal margin of the optic disc on radial B scans (Figs. 2A4, 2B4).[16,36–41] The horizontal and vertical optic disc tilt angles were defined as the tilt angle along the FoBMO axis and that along the FoBMO vertical axis, respectively. Inferotemporal tilt was recorded with a positive value, and superonasal tilt with a negative value.[36] The optic disc torsion angle was determined as the degree of deviation of the long axis of the optic disc from the reference line perpendicular to the foBMO axis (Figs. 2A3, 2B3).[37,41,42] Inferotemporal torsions relative to the reference line were recorded with a positive value and superonasal torsions with a negative value.[43] The ovality index was measured as the ratio of the largest-to-smallest optic disc diameter.[32,37]

Statistical Analysis

Baseline characteristics and test results were compared among the three groups. One-way ANOVA was used to compare continuous variables among the three groups. Tukey's multiple comparison tests were performed to adjust

for multiple comparisons between groups within each analysis. The categorical variables were analyzed using the χ^2 test when ≤20% of cells have an expected frequency <5.[44] To determine interobserver agreement in assessing MvD-D, MvD-P, or focal LC defects, the kappa coefficient was calculated. The values of temporal width of βPPA$_{+BM}$, βPPA$_{-BM}$, horizontal and vertical optic disc tilt angle, optic disc torsion angle, ODVD, and ovality index, as obtained by the two observers, were compared using the intraclass coefficient (ICC) to determine the inter-observer reproducibility. The analyses were performed using MedCalc (MedCalc, Inc., Mariakerke, Belgium), and P values < 0.05 were considered to be statistically significant.

Results

Among the 489 eyes of 489 POAG patients that were initially enrolled, eyes with poor-quality OCTA images (n = 65) and/or observer failure to reach consensus in interpreting OCTA (n = 45) were excluded. Among the remaining 379 eyes eligible for the study 187 eyes (49.3%) had MvD-D.

There was good inter-observer agreement on the assessment of the presence (κ = 0.89) and sectoral location (κ = 0.87) of MvD-D, the presence (κ = 0.91) and sectoral location (κ = 0.90) of MvD-P, and the presence (κ = 0.87) and sectoral location (κ = 0.84) of focal LC defect. There was also good interobserver reproducibility for measurement of the temporal width of βPPA$_{+BM}$ (ICC = 0.95) and βPPA$_{-BM}$ (ICC = 0.98) horizontal (ICC = 0.98) and vertical (ICC = 0.99) optic disc tilt angle, optic disc torsion angle (ICC = 0.97), ovality index (ICC = 0.99), and ODVD of global area (ICC = 0.95), TS (ICC = 0.94), TI (ICC = 0.90), and T (ICC = 0.96) sectors, respectively. Among the 187 eyes with MvD-D, 44 (23.5%), 78 (41.7%), and 65 (34.8%) were categorized as focal temporal MvD-D (Group 1), supero/inferotemporal MvD-D (Group 2), and diffuse temporal MvD-D (Group 3), respectively.

When the baseline characteristics were compared among the three groups (Table 1), significant differences in AXL, number of topical glaucoma medications, untreated IOP, VF mean deviation (MD) and PSD, the RNFL thicknesses and ODVD of all areas were observed (P < 0.05). Multiple comparisons using Tukey's test revealed that the focal temporal MvD-D group (Group 1) had a significantly longer AXL (25.7 ± 1.7 mm) than did the other two groups (cf., 24.6 ± 1.7 mm for Group 2 and 24.4 ± 1.5 mm for Group 3) (P < 0.001) (Table 1). Moreover, Group 1 (49.7 ± 12.1 µm for RNFL thickness and 56.3% ± 12.9% for ODVD) had a significantly thinner RNFL and lower ODVD in the temporal sector than did Group 2 (58.5 ± 11.3 µm RNFL thickness and 66.9% ± 15.0% for ODVD), despite similar RNFL thicknesses in the global area and all other sectors (Table 1, Figs. 2A5, 2A6, 2B5, 2B6). Group 3 had a significantly larger number of glaucoma medications, higher untreated IOP, worse MD and PSD, thinner RNFL in the global area, NI, NS, and TI sectors, and lower ODVD in all areas than did the other two groups, as well as thinner RNFL in the N, T, and TS sectors than Group 2 (P < 0.05) (Table 1). Age differed marginally (P = 0.090). No other factors, including gender, central corneal thickness, IOP at scan time, systolic BP, diastolic BP, mean ocular perfusion pressure, presence of pre-perimetric POAG, and disc hemorrhage, differed among the three groups (P > 0.10).

When the parameters of optic disc morphology were compared among the three groups (Table 2), Group 1 had significantly longer temporal βPPA$_{-BM}$ width (437.4 ± 330.8 µm), larger horizontal optic disc tilt angle (15.9° ± 11.9°), and larger ovality index (1.3 ± 0.2) than did the other two groups (147.6 ± 205.0 µm for βPPA$_{-BM}$ width, 6.1° ± 6.8° for horizontal optic disc tilt angle, and 1.1 ± 0.1 for ovality index for Group 2; 167.9 ± 240.1 µm for βPPA$_{-BM}$ width, 7.2° ± 8.4° for horizontal optic disc tilt angle, 1.1 ± 0.1 for ovality index for Group 3) (P < 0.05). Temporal βPPA$_{+BM}$ width was significantly larger in Group 2 than in Group 3 (337.0 ± 180.7 µm vs. 256.8 ± 134.9 µm; P = 0.012). The three groups did not differ in terms of BMO area, vertical optic disc tilt angle, optic disc torsion angle or the presence of MvD-P and focal LC defect (P > 0.05).

MvD-D was detected in only 1 sector in 121 eyes (64.7%) and in ≥2 sectors in 66 eyes (35.3%). The percentage of eyes with multiple MvD-D was significantly lower in Group 2 (16.7% [13/78]) than in the other two groups (54.5% [24/44] for Group 1; 44.6% [29/65] for Group 3) (P < 0.001) (Table 2).

MvD-P was present in 81.8% (36/44), 89.7% (70/78), and 87.7% (57/65) of Group 1, 2, and 3 eyes, respectively (P = 0.676) (Table 2). All eyes of the three groups having both MvD-D and MvD-P had ≥1 sector, of which both types of dropout were present.

Focal LC defect was present in 72.7% (32/44), 75.6% (59/78), and 75.4% (49/65) of Group 1, 2, and 3 eyes, respectively (P = 0.931) (Table 2). Eyes of Group 1 having both MvD-D and focal LC defect showed a significantly lower percentage of eyes (59.4% [19/32]) having ≥1 sector in which both MvD-D and focal LC defects were present than did Group 2 (96.7% [57/59]) and Group 3 (100% [49/49]) (P < 0.001).

Discussion

The present study categorized the circumferential location of MvD-D by SS-OCTA and associated optic disc morphological characteristics. We found that eyes with focal temporal MvD-D had longer AXL and βPPA$_{-BM}$, as well as larger optic disc tilt angle and ovality index than did the other types of MvD-D. This result suggests that focal temporal MvD-D may be related to a different pathogenic mechanism than that of typical MvD-D located mainly in the inferotemporal or superotemporal areas of the ONH.[13,15]

Given that typical glaucomatous ONH damage develops preferentially in the inferotemporal and superotemporal areas due to weak structural support of the LC in those areas,[33,34,45,46] it is plausible that MvD-D also develops preferentially in these areas.[13] Therefore the temporal area of the ONH is likely to be preserved until the moderate-to-advanced stages of glaucoma. Similarly, in this study, the diffuse temporal MvD-D group showed the worst disease severity among the three groups.[45] In contrast, the focal temporal MvD-D group was localized to the temporal area despite relatively early disease severity, and a relatively high percentage of multiple MvD-D was observed in focal temporal MvD-D group. Moreover, these eyes exhibited eye globe elongation, a longer scleral flange, and increased tilting and ovality of the optic disc. This suggests that the pathogenic mechanism of focal temporal MvD-D could be the tensile strength exerted in the temporal area of the ONH, as originating from axial elongation and subsequent deformation of the parapapillary region. Although the underlying pathogenesis is uncertain, a number of studies have reported that the temporal region is vulnerable to myopic alteration of

Investigative Ophthalmology & Visual Science

Table 1. Comparison of the Baseline Characteristics Among the Three Groups According to the Circumferential Location of the MvD-D

Variables	Group 1 (Focal Temporal MvD-D)	Group 2 (Supero/Inferotemporal MvD-D)	Group 3 (Diffuse Temporal MvD-D)	*P* Value	Post Hoc‡
N	44	78	65		
Age (yr)	52.5 ± 13.4	56.9 ± 13.5	58.2 ± 13.3	0.090*	
Gender				0.426†	
Male	24	33	31		
Female	20	45	34		
Axial length (mm)	25.7 ± 1.7	24.6 ± 1.7	24.4 ± 1.5	**<0.001***	2, 3 < 1
CCT (µm)	535.9 ± 42.9	531.9 ± 31.5	534.2 ± 28.7	0.810*	
Self-reported diabetes	4 (9.1%)	8 (10.3%)	7 (10.8%)	0.960†	
Self-reported hypertension	6 (13.6%)	16 (20.5%)	15 (23.1%)	0.468†	
Diabetes medication	4 (9.1%)	8 (10.3%)	7 (10.8%)	0.960†	
Antihypertensive medication	6 (13.6%)	14 (17.9%)	14 (21.5%)	0.575†	
Number of topical glaucoma medications				**0.001**†	1,2 < 3
≤1	26 (59.1%)	38 (48.7%)	17 (26.2%)		
>1	18 (40.9%)	40 (51.3%)	48 (73.8%)		
Topical medications				0.981†	
Prostaglandin analogues	27	52	53		
Beta-antagonists	30	52	50		
Carbonic anhydrase inhibitors	25	47	50		
Alpha-1-agonists	13	27	32		
Untreated IOP (mm Hg)	16.3 ± 3.1	16.2 ± 3.1	18.9 ± 6.9	**0.002***	1, 2 < 3
IOP at scan time (mm Hg)	11.7 ± 2.4	11.7 ± 2.0	12.1 ± 2.2	0.423*	
Disc hemorrhage	6 (13.6%)	22 (28.2%)	13 (20.0%)	0.157†	
Visual Field MD (dB)	−5.2 ± 3.8	−6.7 ± 5.4	−11.2 ± 6.9	**<0.001***	3 < 1, 2
Visual Field PSD (dB)	5.9 ± 3.7	7.3 ± 4.2	9.0 ± 4.1	**0.001***	1, 2 < 3
Type of POAG (Pre-perimetric/Perimetreic)	3/41	3/75	2/63	0.829‡	
RNFL thickness (µm)					
Average	68.0 ± 13.1	71.9 ± 11.4	59.4 ± 12.4	**<0.001***	3 < 1, 2
N	60.7 ± 19.3	65.7 ± 12.2	57.4 ± 15.5	**0.006***	3 < 2
NI	78.0 ± 19.0	77.9 ± 20.2	63.2 ± 23.2	**<0.001***	3 < 1, 2
NS	97.9 ± 29.0	94.6 ± 31.1	81.9 ± 29.7	**0.010***	3 < 1, 2
T	49.7 ± 12.1	58.5 ± 11.3	45.6 ± 12.7	**<0.001***	1, 3 < 2
TI	66.6 ± 33.2	66.1 ± 27.7	55.0 ± 25.2	**0.036***	3 < 1, 2
TS	91.0 ± 35.3	97.6 ± 33.9	75.2 ± 30.0	**0.001***	3 < 2
Optic disc vessel density (%)					
Average	54.1% ± 10.8%	57.1% ± 11.5%	40.1% ± 12.15%	**<0.001***	3 < 1, 2
T	56.3% ± 12.9%	66.9% ± 15.0%	41.5% ± 14.2%	**<0.001***	3 < 1 < 2
TI	49.3% ± 13.4%	46.4% ± 12.8%	37.9% ± 12.8%	**<0.001***	3 < 1, 2
TS	52.5% ± 13.0%	54.8% ± 14.0%	41.9% ± 14.2%	**<0.001***	3 < 1, 2

CCT, central corneal thickness; N, nasal; NI, nasal inferior; NS, nasal superior; T, temporal.
Values are means ± standard deviation unless otherwise indicated. *P* values < 0.05 are noted in boldface.
* The comparison was performed by using one-way analysis of variance.
† The comparison was performed by using chi-square test.
‡ Significance based on the Tukey-Kramer honest significant difference (HSD) post hoc test.

the optic disc.[15,47–50] The current study adds to the literature that OCTA-derived focal temporal MvD-D can be a potential marker of mechanical strain in the corresponding temporal area of the ONH.

Similarly, the focal temporal MvD-D group showed a thinner RNFL of the corresponding temporal sector in relation to the supero/inferotemporal MvD-D group, despite similar RNFL thicknesses in all other areas. These findings concur with previous reports that localized papillomacular bundle defects were frequently observed in highly myopic eyes.[51,52] However, the present study did not assess the pattern of VF damage, because it had included both pre-perimetric and perimetric POAG patients. Also, all eyes had MvD-D, and in most of those cases (87.2%), MvD-P as well. Given that a number of studies have reported that eyes with MvD-P tended to have paracentral scotoma on VF tests,[53,54] it is likely that the three groups have paracentral involvement. Future studies on the involvement of parafoveal VF defects according to the presence of MvD-D are warranted.

One may that argue supero/inferotemporal MvD-D may be derived by axial elongation if the mechanical stretching is focally on these areas. However, it is less likely that the tractional force is only in the TS or TI areas during axial elongation. A recent study showing that the extent of central retinal vascular trunk dragging during eye globe elongation was less than 30° supports this notion.[55]

Investigative Ophthalmology & Visual Science

Table 2. Comparison of the Morphological Parameters of the Optic Disc Among the 3 Groups According to the Circumferential Location of the MvD-D

Variables	Group 1 (Focal Temporal MvD-D)	Group 2 (Supero/Inferotemporal MvD-D)	Group 3 (Diffuse Temporal MvD-D)	*P* Value	Post Hoc‡
N	44	78	65		
BMO area (mm^2)	2.5 ± 0.8	2.4 ± 0.6	2.6 ± 0.6	0.343*	
Temporal βPPA_{+BM} width (μm)	311.4 ± 160.0	337.0 ± 180.7	256.8 ± 134.9	**0.012***	2 > 3
Temporal βPPA_{-BM} width (μm)	437.4 ± 330.8	147.6 ± 205.0	167.9 ± 240.1	**<0.001***	2,3 <1
Horizontal optic disc tilt angle	15.9° ± 11.9°	6.1° ± 6.8°	7.2° ± 8.4°	**<0.001***	2,3 <1
Vertical optic disc tilt angle	2.8° ± 5.2°	3.9° ± 5.3°	3.7° ± 5.5°	0.477*	
Optic disc torsion angle	8.7° ± 11.9°	5.1° ± 9.6°	5.0° ± 12.5°	0.180*	
Ovality index	1.3 ± 0.2	1.1° ± 0.1°	1.1° ± 0.1°	**<0.001***	2,3 <1
Presence of multiple MvD-D	24 (54.5%)	13 (16.7%)	29 (44.6%)	**<0.001***	2<1, 3
Presence of the MvD-P	36 (81.8%)	70 (89.7%)	57 (87.7%)	0.676†	
Presence of the focal LC defect	32 (72.7%)	59 (75.6%)	49 (75.4%)	0.931†	

Values are means ± standard deviation unless otherwise indicated. *P* values < 0.05 are noted in boldface.
* The comparison was performed by using one-way analysis of variance.
† The comparison was performed by using chi-square test.
‡ Significance based on the Tukey-Kramer honest significant difference (HSD) post hoc test.

In this study, optic disc microvasculature was assessed both quantitatively and quantitatively. Focal temporal MvD-D group had significantly lower ODVD than supero/inferotemporal MvD-D group in the temporal area, despite similar values in the global area and TS and TI sectors. This finding suggests that both quantitative and qualitative analyses of the MvD-D had consistent results. In particular, qualitative analysis of the horizontal B scan images of the OCTA helps assess the deep ONH vasculature under the neuroretinal rim area. Eyes with visible laminar vasculature on the horizontal B scan, despite shadowing of the neuroretinal rim, were categorized as those without MvD-D (Fig. 1B) In contrast, eyes with distinctive loss of laminar vasculature were categorized as those with MvD-D (Fig. 1C). Eyes with indiscernible MvD-D in which the anterior LC was not visualized because of shadowing in the horizontal B scan were excluded (Fig. 1A).[13] However, it is difficult to differentiate the three cases based on the quantitative analysis which utilized only en-face OCTA images. After excluding the neuroretinal rim, the optic disc cup was assessed on the quantitative analysis. This suggests that qualitative and quantitative analysis can complement assessing MvD-D.

The degree of optic disc torsion has been determined to have an important role in myopic optic disc change in previous studies.[16,37,42,56,57] Although the current study's focal temporal MvD-D group tended to have a larger degree of torsion than the other two groups, the differences did not reach statistical significance. This finding may be attributable to the relatively smaller differences of mean AXL among the three groups (25.7 mm in the focal temporal MvD-D group vs. approximately 24.5 mm in the other two groups) compared with those of previous studies (approximately 26.2 mm in myopic eyes vs. approximately 23.2 mm in non-myopic eyes).[42,57] Inclusion of greater numbers of highly myopic eyes in future studies may help to elucidate the association between the circumferential location of MvD-D and optic disc torsion.

Previous studies found MvD-D to be closely associated with both focal LC defect and MvD-P.[7,13] For the supero/inferotemporal and diffuse temporal MvD-D groups of the present study, MvD-D had a close topographical relationship with both MvD-P and focal LC defect; the focal temporal MvD-D group, however, showed a lesser topographical relationship with focal LC defect (59.4% vs. 96.6% for the supero/inferotemporal MvD-D group and 100% for the diffuse temporal MVD-D group; $P < 0.001$), despite the close topographical relationship between MvD-D and MvD-P (100% for all three groups). This result does not correspond with previous studies in which temporal focal LC defect was frequently observed in myopic eyes.[15,32,55] Given that MvD-D and focal LC defect share a pathogenic mechanism (i.e., axial elongation),[15,32,55] further investigations are needed to elucidate the discrepancy between the two features observed in the present study.

The current result that the diffuse MvD-D group had significantly worse disease severity, higher untreated IOP, and tended to be older in age than the other two groups is consistent with previous studies reporting that the extent of structural and vascular ONH damage grows as glaucoma progresses.[46,58,59] Meanwhile, the finding that the diffuse MvD-D group had smaller ßPPA$_{+BM}$ than did the supero/inferotemporal MvD-D group is not consistent with previous findings that ßPPA$_{+BM}$ width was related to older age and worse disease severity.[29] It is unclear whether this was due to the population differences across studies.

A control group not having MvD-D was not included in this study. When the analysis was performed after including the control group, VF parameters and RNFL thicknesses of the control group were better than the other three groups in most areas (Supplemental Table S1). Therefore inclusion of a control group does not provide meaningful information and rather leads to confusion in investigating the clinical characteristics of focal temporal MvD-D group.

The present study has several limitations. First, the number of eligible eyes with focal temporal MvD-D was relatively small ($n = 44$). However, the total number of subjects ($n = 187$) showed acceptable power (0.87) and effect size f (0.25) for detecting significant differences of key parameters (i.e., AXL, RNFL thickness, and ODVD) across the three groups. Second, although the assessment of MvD-

D and MvD-P was performed during separate sessions, the observers were not masked to MvD-D when evaluating MvD-P and vice versa, because the current OCTA device does not provide for masking of the parapapillary and optic disc areas. This may have led to bias in determining MvD-D and MvD-P. Third, we used width of βPPA, angle of optic disc tilt and torsion to assess the degree of morphological parapapillary-ONH changes derived by axial elongation, as based on a number of previous publications.[16,36–41] Recently, 3-dimensional ONH parameters (i.e., anterior scleral canal opening/BMO offset magnitude, position of vascular trunk) have been proposed as potential landmarks, although accurate segmentation of these features is often challenging.[49,55,60] Improvement of OCT technology is called for to provide for better segmentation of parapapillary ONH structures including the anterior scleral canal opening and BMO. Fourth, given that this study is cross-sectional in nature, the temporal relationship between the MvD-D and myopic structural change is unclear. Although it is more likely that MvD-D is derived by axial elongation and subsequent optic disc changes, longitudinal studies are needed to evaluate the temporal relationship between MVD and optic disc changes. Also, only glaucomatous eyes were included in this study, thus further investigation on the healthy myopic eyes are needed to reinforce the hypothesis. However, possible influencing factors on the MvD-D (i.e., disease severity, presence of focal LC defect, and MvD-P) did not differ between focal temporal MvD-D and supero/inferotemporal MvD-D groups. Finally, our recent study reported that the optic disc size affects the visualization of MvD-D.[13] Although the BMO areas did not differ across the three groups, there may have been a preference for selecting eyes with larger discs, leading to potential selection bias.

In conclusion, MvD-D localized to the temporal area was well characterized by utilizing SS-OCTA. Focal temporal MvD-D was associated with longer AXL and βPPA without BM, as well as large optic disc tilt angle and ovality index. These findings suggest that tensile strength exerted in the temporal optic disc as originating from elongation of the globe may lead to the focal absence of temporal optic disc microvasculature. Longitudinal studies are needed to assess the pathogenic role of focal temporal MvD-D in glaucoma development and progression.

Acknowledgments

The authors thank Do Hee Jung, MD for his data acquisition.

Supported in part by National Eye Institute (R01EY029058) and an unrestricted grant by Research to Prevent Blindness (New York, NY).

Disclosure: **Y.J. Lim**, None; **J.W. Bang**, None; **R.N. Weinreb**, None; **L.M. Zangwill**, None; **M.H. Suh**, None

References

1. Weinreb RN, Aung T, Medeiros FA. The pathophysiology and treatment of glaucoma: a review. *JAMA*. 2014;311:1901–1911.
2. Fechtner RD, Weinreb RN. Mechanisms of optic nerve damage in primary open angle glaucoma. *Surv Ophthalmol*. 1994;39:23–42.
3. Flammer J. The vascular concept of glaucoma. *Surv Ophthalmol*. 1994;38:S3–S6.
4. Weinreb RN, Harris A. *Ocular Blood Flow in Glaucoma*. Vol. 6. Amsterdam: Kugler Publications; 2009.
5. Hayreh SS. Blood supply of the optic nerve head and its role in optic atrophy, glaucoma, and oedema of the optic disc. *Br J Ophthalmol*. 1969;53:721.
6. Anderson DR, Braverman S. Reevaluation of the optic disk vasculature. *Am J Ophthalmol*. 1976;82(2):165–174.
7. Onda E, Cioffi GA, Bacon DR, van BUSKIRK EM. Microvasculature of the human optic nerve. *Am J Ophthalmol*. 1995;120:92–102.
8. Suh MH, Zangwill LM, Manalastas PIC, et al. Deep retinal layer microvasculature dropout detected by the optical coherence tomography angiography in glaucoma. *Ophthalmology*. 2016;123:2509–2518.
9. Akagi T, Zangwill LM, Shoji T, et al. Optic disc microvasculature dropout in primary open-angle glaucoma measured with optical coherence tomography angiography. *PLoS One*. 2018;13(8):e0201729.
10. Kim JA, Kim TW, Lee EJ, Girard MJA, Mari JM. Relationship between lamina cribrosa curvature and the microvasculature in treatment-naïve eyes. *Br J Ophthalmol*. 2020;104:398–403.
11. Kim JA, Kim TW, Lee EJ, Girard MJA, Mari JM. Microvascular changes in peripapillary and optic nerve head tissues after trabeculectomy in primary open-angle glaucoma. *Invest Ophthalmol Vis Sci*. 2018;59:4614–4621.
12. Lee EJ, Kim TW, Weinreb RN, Park KH, Kim SH, Kim DM. Visualization of the lamina cribrosa using enhanced depth imaging spectral-domain optical coherence tomography. *Am J Ophthalmol*. 2011;152:87–95.
13. Suh MH, Jung DH, Weinreb RN, Zangwill LM. Optic disc microvasculature dropout in glaucoma detected by swept-source optical coherence tomography angiography. *Am J Ophthalmol*. 2022;236:261–270.
14. Numa S, Akagi T, Uji A, et al. Visualization of the lamina cribrosa microvasculature in normal and glaucomatous eyes: a swept-source optical coherence tomography angiography study. *J Glaucoma*. 2018;27:1032–1035.
15. Sawada Y, Araie M, Ishikawa M, Yoshitomi T. Multiple temporal lamina cribrosa defects in myopic eyes with glaucoma and their association with visual field defects. *Ophthalmology*. 2017;124:1600–1611.
16. Kimura Y, Akagi T, Hangai M, et al. Lamina cribrosa defects and optic disc morphology in primary open angle glaucoma with high myopia. *PLoS One*. 2014;9(12):e115313.
17. Sample PA, Girkin CA, Zangwill LM, et al. The African descent and glaucoma evaluation study (ADAGES): design and baseline data. *Arch Ophthalmol*. 2009;127:1136–1145.
18. Kwon JM, Weinreb RN, Zangwill LM, Suh MH. Juxtapapillary deep-layer microvasculature dropout and retinal nerve fiber layer thinning in glaucoma. *Am J Ophthalmol*. 2021;227:154–165.
19. Meditec CZ. *Carl Zeiss Meditec Plex Elite 9000 OCT 501(k) Premarket Report of FDA 2016*.
20. Chu Z, Weinstein JE, Wang RK, Pepple KL. Quantitative analysis of the choriocapillaris in uveitis using en face swept-source optical coherence tomography angiography. *Am J Ophthalmol*. 2020;218:17–27.
21. Shen M, Zhang Q, Yang J, et al. Swept-source OCT angiographic characteristics of treatment-naive nonexudative macular neovascularization in AMD prior to exudation. *Invest Ophthalmol Vis Sci*. 2021;62(6):14.
22. Miller AR, Roisman L, Zhang Q, et al. Comparison between spectral-domain and swept-source optical coherence tomography angiographic imaging of choroidal neovascularization. *Invest Ophthalmol Vis Sci*. 2017;58:1499–1505.

23. Kwon JM, Weinreb RN, Zangwill LM, Suh MH. Parapapillary deep-layer microvasculature dropout and visual field progression in glaucoma. *Am J Ophthalmol*. 2019;200:65–75.
24. Park JW, Suh MH, Agrawal R, Khandelwal N. Peripapillary choroidal vascularity index in glaucoma—a comparison between spectral-domain OCT and OCT angiography. *Invest Ophthalmol Vis Sci*. 2018;59:3694–3701.
25. Chauhan BC, Burgoyne CF. From clinical examination of the optic disc to clinical assessment of the optic nerve head: a paradigm change. *Am J Ophthalmol*. 2013;156:218–227.
26. Al-Sheikh M, Ghasemi Falavarjani K, Akil H, Sadda SR. Impact of image quality on OCT angiography based quantitative measurements. *Int J Retin Vitr*. 2017;3:1–6.
27. Al-Sheikh M, Akil H, Pfau M, Sadda SR. Swept-source OCT angiography imaging of the foveal avascular zone and macular capillary network density in diabetic retinopathy. *Invest Ophthalmol Vis Sci*. 2016;57:3907–3913.
28. Sadda SR, Wu Z, Walsh AC, et al. Errors in retinal thickness measurements obtained by optical coherence tomography. *Ophthalmology*. 2006;113:285–293.
29. Kim M, Kim TW, Weinreb RN, Lee EJ. Differentiation of parapapillary atrophy using spectral-domain optical coherence tomography. *Ophthalmology*. 2013;120:1790–1797.
30. Kim HR, Weinreb RN, Zangwill LM, Suh MH. Characteristics of focal gamma zone parapapillary atrophy. *Invest Ophthalmol Vis Sci*. 2020;61(3):17.
31. Suh MH, Zangwill LM, Manalastas PIC, et al. Deep-layer microvasculature dropout by optical coherence tomography angiography and microstructure of parapapillary atrophy. *Invest Ophthalmol Vis Sci*. 2018;59:1996–2005.
32. Sawada Y, Araie M, Kasuga H, et al. Focal lamina cribrosa defect in myopic eyes with nonprogressive glaucomatous visual field defect. *Am J Ophthalmol*. 2018;190:34–49.
33. Tatham AJ, Miki A, Weinreb RN, Zangwill LM, Medeiros FA. Defects of the lamina cribrosa in eyes with localized retinal nerve fiber layer loss. *Ophthalmology*. 2014;121:110–118.
34. Suh MH, Zangwill LM, Manalastas PIC, et al. Optical coherence tomography angiography vessel density in glaucomatous eyes with focal lamina cribrosa defects. *Ophthalmology*. 2016;123:2309–2317.
35. Kiumehr S, Park SC, Dorairaj S, et al. In vivo evaluation of focal lamina cribrosa defects in glaucoma. *Arch Ophthalmol*. 2012;130:552–559.
36. Park HYL, Il Choi S, Choi JA, Park CK. Disc torsion and vertical disc tilt are related to subfoveal scleral thickness in open-angle glaucoma patients with myopia. *Invest Ophthalmol Vis Sci*. 2015;56:4927–4935.
37. Kim YC, Moon JS, Park HYL, Park CK. Three dimensional evaluation of posterior pole and optic nerve head in tilted disc. *Sci Rep*. 2018;8:1–11.
38. Choi JH, Han JC, Kee C. The effects of optic nerve head tilt on visual field defects in myopic normal tension glaucoma: the intereye comparison study. *J Glaucoma*. 2019;28:341–346.
39. Hosseini H, Nassiri N, Azarbod P, et al. Measurement of the optic disc vertical tilt angle with spectral-domain optical coherence tomography and influencing factors. *Am J Ophthalmol*. 2013;156:737–744.
40. Takasaki H, Higashide T, Takeda H, Ohkubo S, Sugiyama K. Relationship between optic disc ovality and horizontal disc tilt in normal young subjects. *Jpn J Ophthalmol*. 2013;57:34–40.
41. Jeon SJ, Park HYL, Kim YC, Kim EK, Park CK. Association of scleral deformation around the optic nerve head with central visual function in normal-tension glaucoma and myopia. *Am J Ophthalmol*. 2020;217:287–296.
42. Park HYL, Lee K, Park CK. Optic disc torsion direction predicts the location of glaucomatous damage in normal-tension glaucoma patients with myopia. *Ophthalmology*. 2012;119:1844–1851.
43. Araie M, Iwase A, Sugiyama K, et al. Determinants and characteristics of Bruch's membrane opening and Bruch's membrane opening–minimum rim width in a normal Japanese population. *Invest Ophthalmol Vis Sci*. 2017;58(10):4106–4113.
44. Nowacki A. Chi-square and Fisher's exact tests. *Cleve Clin J Med*. 2017;84(9 suppl 2):e20–e25.
45. Leung CKS, Choi N, Weinreb RN, et al. Retinal nerve fiber layer imaging with spectral-domain optical coherence tomography: pattern of RNFL defects in glaucoma. *Ophthalmology*. 2010;117:2337–2344.
46. Suh MH, Kim DM, Kim YK, Kim TW, Park KH. Patterns of progression of localized retinal nerve fibre layer defect on red-free fundus photographs in normal-tension glaucoma. *Eye*. 2010;24:857–863.
47. Kim TW, Kim M, Weinreb RN, Woo SJ, Park KH, Hwang JM. Optic disc change with incipient myopia of childhood. *Ophthalmology*. 2012;119:21–26.
48. Kim M, Choung HK, Lee KM, Oh S, Kim SH. Longitudinal changes of optic nerve head and peripapillary structure during childhood myopia progression on OCT: Boramae Myopia Cohort Study Report 1. *Ophthalmology*. 2018;125:1215–1223.
49. Jeoung JW, Yang H, Gardiner S, et al. Optical coherence tomography optic nerve head morphology in myopia I: implications of anterior scleral canal opening versus Bruch membrane opening offset. *Am J Ophthalmol*. 2020;218:105–119.
50. Jonas JB, Wang YX, Dong L, Guo Y, Panda-Jonas S. Advances in myopia research anatomical findings in highly myopic eyes. *Eye Vis*. 2020;7:1–10.
51. Kimura Y, Hangai M, Morooka S, et al. Retinal nerve fiber layer defects in highly myopic eyes with early glaucoma. *Invest Ophthalmol Vis Sci*. 2012;53:6472–6478.
52. Greve EL, Furuno F. Myopia and glaucoma. *Graefes Arch Exp Ophthalmol*. 1980;213:33–41.
53. Lee EJ, Kim TW, Kim JA, Kim JA. Central visual field damage and parapapillary choroidal microvasculature dropout in primary open-angle glaucoma. *Ophthalmology*. 2018;125(4):588–596.
54. Kwon J, Shin JW, Lee J, Kook MS. Choroidal microvasculature dropout is associated with parafoveal visual field defects in glaucoma. *Am J Ophthalmol*. 2018;188:141–154.
55. Lee KM, Choung HK, Kim M, Oh S, Kim SH. Positional change of optic nerve head vasculature during axial elongation as evidence of lamina cribrosa shifting: Boramae Myopia Cohort Study Report 2. *Ophthalmology*. 2018;125(8):1224–1233.
56. Lee KS, Lee JR, Kook MS. Optic disc torsion presenting as unilateral glaucomatous-appearing visual field defect in young myopic Korean eyes. *Ophthalmology*. 2014;121:1013–1019.
57. Park HYL, Lee KI, Lee K, Shin HY, Park CK. Torsion of the optic nerve head is a prominent feature of normal-tension glaucoma. *Invest Ophthalmol Vis Sci*. 2015;56:156–163.
58. Song MK, Shin JW, Lee JY, Hong JW, Kook MS. Choroidal microvasculature dropout is spatially associated with optic nerve head microvasculature loss in open-angle glaucoma. *Sci Rep*. 2021;11:1–9.
59. Kim JA, Lee EJ, Kim TW. Evaluation of parapapillary choroidal microvasculature dropout and progressive retinal nerve fiber layer thinning in patients with glaucoma. *JAMA Ophthalmol*. 2019;137:810–816.
60. Rezapour J, Bowd C, Dohleman J, et al. The influence of axial myopia on optic disc characteristics of glaucoma eyes. *Sci Rep*. 2021;11(1):1–13.

Investigative Ophthalmology & Visual Science